PRAMANA
— journal of
physics

Vol. 71, No. 2
August 2008
pp. 211–232

Solvent density mode instability in non-polar solutions

SUSMITA KAR[1], RANJIT BISWAS[1,2,*] and J CHAKRABARTI[1,3,*]
[1]Department of Chemical, Biological and Macromolecular Sciences, S. N. Bose National Centre for Basic Sciences, JD Block, Salt Lake City, Kolkata 700 098, India
[2]Also at the Unit for Nanoscience and Technology, S.N. Bose National Centre for Basic Sciences, JD Block, Salt Lake City, Kolkata 700 098, India
[3]Also at the Advanced Materials Research Unit, S.N. Bose National Centre for Basic Sciences, JD Block, Salt Lake City, Kolkata 700 098, India
*Corresponding authors
E-mail: ranjit@bose.res.in; jaydeb@bose.res.in

Abstract. We analyse the origin of the multiple long time scales associated with the long time decay observed in non-polar solvation dynamics by linear stability analysis of solvent density modes where the effects of compressibility and solvent structure are systematically incorporated. The coupling of the solute–solvent interactions at both ground and excited states of the solute with the compressibility and solvent structure is found to have important effects on the time scales. The present theory suggests that the relatively longer time constant is controlled by the solvent compressibility, while the solvent structure at the nearest-neighbour length scale dominates the shorter time constant.

Keywords. Linear stability; non-polar solvation dynamics; solvation time scale.

PACS Nos 31.70.Dk; 64.70.Fx; 78.47.+p

1. Introduction

The rate of a chemical reaction in solution phase is controlled by many factors such as the activation energy, the nature of the reaction potential energy surface, vibrational energy of a bond, the viscosity of the reaction medium, the distribution of the solvent molecules around the reactant particles, i.e. solvent caging, the polarity of the solvent etc. [1–5]. Among these factors, the distribution of the solvent molecules is of fundamental importance as the solvent rearrangement governs the rate by affecting the stabilization of the relevant transition state and subsequently the product [6–9]. The time-dependent rearrangement of the solvent molecules around an excited solute is known as solvation dynamics. Therefore, dynamical solvent control of a reaction by the solvent in solution can be understood by following the solvation dynamics of the reaction medium.

Experimentally, the time-dependent progress of solvation of an excited solute is usually followed by monitoring the time-dependent fluorescence Stokes shift (TDFSS) of the emission spectrum of a solute dissolved in a solvent [6]. In the case of polar solvation, a dipolar solute dissolved in a polar solvent is excited by an intense laser pulse [6]. A large dipole moment is thus created instantaneously in the excited state of the solute. Therefore, immediately after the excitation (that is, at $t = 0$) the solvent distribution around the excited solute is the same as that when the solute was in its ground state [6]. This is a non-equilibrium situation that drives the neighbouring solvent molecules to rotate and translate in order to minimize the free energy so that a new equilibrium state is reached [4,6,10,11]. In time-resolved fluorescence experiments, the entire process of solvent rearrangement around the excited solute is monitored via the solvent response function [4,6], i.e., $S(t) = (\nu(t) - \nu(\infty))/(\nu(0) - \nu(\infty))$, where $\nu(t)$ denotes the peak frequency of the time-dependent fluorescence emission spectrum of the solute probe, $\nu(0)$ denotes the emission peak frequency immediately after the excitation and $\nu(\infty)$ represents the emission peak frequency of the solute after the solvent redistribution is complete and hence, should be the same as that obtained from the steady state fluorescence emission studies [6]. Note that $S(t)$ is so normalized that it decays from unity at $t = 0$ to zero at $t = \infty$.

In the case of non-polar solvation, the change in shape and size of the solute upon excitation mainly drives the solvent reorganization [12,13]. However, the Stokes shifts associated with such processes are always less than 500 cm^{-1} and hence, results obtained by using the TDFSS techniques are not always reliable [13]. This difficulty is partially solved by studying solvation dynamics of a dipolar probe in non-dipolar solvents. In these cases, the magnitude of Stokes shift is relatively larger because of the additional coupling of the instantaneously changed solute dipole moment with the electronic polarizability of the solvent molecules [13]. However, the magnitude of the dynamic Stokes shift in non-dipolar solvation is smaller by at least a factor of 2 than that for dipolar solute in dipolar solvent cases. Interestingly, non-polar solvation contributes significantly in non-dipolar solvation because the translational motion of the solvent molecules controls a substantial portion of the total solvation energy relaxation. Therefore, a molecular level understanding of non-polar solvation dynamics is necessary for systems where coupling of the solute–solvent non-polar interactions with various solvent modes (for example, compressibility and nearest-neighbour arrangements) are expected to play a very significant role.

Since time-dependent solvation energy is essentially the difference in energies due to the interaction of solvent molecules with the solute in its excited and ground states, the solvent response function can also be expressed as [14–16] $S(t) = (\Delta E(t) - \Delta E(\infty))/(\Delta E(0) - \Delta E(\infty))$, where $\Delta E(t)$ is the time-dependent solvation energy gap with respect to the ground state of the solute. Let the interaction between the solute (u) at $\underline{R}$ and a solvent (v) at $\underline{r}$ in the ground state of the solute be $V_{uv}^{\mathrm{gs}}(\underline{r} - \underline{R})$. Assuming that the solute–solvent interaction becomes $V_{uv}^{\mathrm{ex}}(\underline{r} - \underline{R})$ upon solute excitation, leading to the solvent rearrangement, we get $\Delta E(t) = \int \mathrm{d}\underline{r}[V_{uv}^{\mathrm{ex}}(\underline{r} - \underline{R})\rho(\underline{r}, t) - V_{uv}^{\mathrm{gs}}(\underline{r} - \underline{R})\rho_{\mathrm{gs}}(\underline{r})]$ where $\rho_{\mathrm{gs}}(\underline{r})$ is the solvent density in equilibrium with the solute in the ground state [17]. Thus the solvent response function is related to the time-dependent density fluctuation of the solvent

around the solute which can be accounted for by applying the dynamical density functional theory approach.

We would like to mention here that non-polar solvation dynamics has been studied earlier by using theories based on the linear response of the time-dependent density via the dynamic structure factor [12,18], and also using the full solution of the non-linear hydrodynamic equations (NLHE) for the time-dependent density $\rho(\underline{r}, t)$ [15]. However, these theories report, in addition to one ultra-fast (subpicoseconds) time scale, only one long time scale for the solvation. Experiments, on the other hand, report multiple time scales for the solvation energy relaxation at long times [13]. The microscopic origin of these time scales is still not properly understood. Recently, Biswas and Chakrabarti [17] have shown that the multiple long time scales may be understood as instability time scales [19] of the density modes in the non-linear hydrodynamic equation in the presence of the ground state inhomogeneity of the solvent distribution. In this paper we attempt to understand the origin of the very long time-scales in terms of solute–solvent interaction where effects of the solvent compressibility and the nearest-neighbour arrangement have been investigated.

The organization of the rest of the paper is as follows. Section 2 describes the general theoretical formulation while §3 contains the application of the theory to non-polar solvation. The results and the discussions are given in §4. We conclude the paper in §5.

2. Theoretical formulation

According to the DFT, the free energy cost of creating density inhomogeneity over a bulk solvent of average density ρ_0 is [20–22]

$$\beta F^{\mathrm{eq}}[\rho(\underline{r})] = \int \mathrm{d}\underline{r}\rho(\underline{r}) \left[\ln \frac{\rho(\underline{r})}{\rho_0} - 1\right] - \frac{1}{2}\int \mathrm{d}\underline{r}\mathrm{d}\underline{r}'\, c(\underline{r}-\underline{r}')[\rho(\underline{r})-\rho_0][\rho(\underline{r}')-\rho_0], \tag{1}$$

where β is the inverse of the Boltzmann constant (k_{B}) times the absolute temperature (T). $\beta F^{\mathrm{eq}}[\rho(\underline{r})]$ is truncated to the second-order in correlation, $c(\underline{r}-\underline{r}')$ denoting the static correlation between two particles at $\underline{r}$ and $\underline{r}'$ in the bulk solvent, assuming that the change in density $\rho(\underline{r}) - \rho_0 \ll \rho_0$.

When a solute particle is added to the solvent, the ground state free energy expression, given in eq. (1), becomes

$$\beta F^{\mathrm{gs}}[\rho(\underline{r})] = \int \mathrm{d}\underline{r}\rho(\underline{r}) \left[\ln\left\{\frac{\rho(\underline{r})}{\rho_0}\right\} - 1\right] - \frac{1}{2}\int \mathrm{d}\underline{r}\,\mathrm{d}\underline{r}'\, c(\underline{r}-\underline{r}')[\rho(\underline{r})-\rho_0][\rho(\underline{r}')-\rho_0] + \beta\int \mathrm{d}r V^{\mathrm{gs}}_{uv}(\underline{r}-\underline{R})\rho(\underline{r}), \tag{2}$$

where $V_{uv}^{\rm gs}(\underline{r}-\underline{R})$ is the ground state potential for the insertion of the solute particle and $c(\underline{r}-\underline{r}')$ is the same as for the bulk case. The fluctuation in the position-dependent solvent density is given as $\delta\rho_{\rm gs}(\underline{r}) = \rho(\underline{r}) - \rho_0$. Putting this in eq. (2) and from the equilibrium condition, $\frac{\delta\beta F^{\rm gs}[\rho(\underline{r})]}{\delta\rho_{\rm gs}(\underline{r})} = 0$, we obtain the following expression for the ground state inhomogeneity in density (up to linear order) due to the insertion of solute particle (see Appendix A for details):

$$\delta\rho_{\rm gs}(\underline{q}) = \frac{-\beta\rho_0 V_{uv}^{\rm gs}(\underline{q})}{1-\rho_0 c(\underline{q})}, \tag{3}$$

where $\delta\rho_{\rm gs}(\underline{q})$ is the wave-number (q)-dependent inhomogeneity in the solvent density associated with the solute in its ground state. Similarly, $c(\underline{q})$ is the wave number-dependent static pair correlation function, obtained by Fourier transforming $c(\underline{r}-\underline{r}')$. $V_{uv}^{\rm gs}(\underline{q})$ denotes the wave number-dependent solute–solvent interaction in the ground state of the solute $V_{uv}^{\rm gs}(\underline{r}-\underline{R})$, setting $\underline{R}=0$.

The time-dependent dynamics of the solvent density $\rho(\underline{r},t)$ is given by the continuity equation [23]

$$\partial_t \rho\,(\underline{r},t) + \underline{\nabla}\cdot\underline{j} = 0, \tag{4}$$

where $\underline{j}$ is the solvent particle current density and $\underline{\nabla}$ denotes the spatial gradient. In the over-damped limit, $\underline{j} = -D\rho(\underline{r},t)\underline{\nabla}(\beta\mu)$, D being the Stokes' diffusion coefficient ($= k_{\rm B}T/3\pi\eta\sigma$) of a solvent molecule with diameter σ in a solvent of viscosity $\eta_{\rm s}$. Here, the chemical potential $\beta\mu = \frac{\delta\beta F[\rho(\underline{r},t)]}{\delta\rho(\underline{r},t)}\cdot\beta F[\rho(\underline{r},t)]$ is the free energy cost of creating non-equilibrium solvent density inhomogeneity over the ground state equilibrium solvent distribution and can be described in terms of the position and time-dependent solvent density in the presence of the ground and excited state solute–solvent interactions as follows:

$$\begin{aligned}\beta F[\rho(\underline{r},t)] = &\int \mathrm{d}\underline{r}\,\rho(\underline{r},t)\left[\ln\left\{\frac{\rho(\underline{r},t)}{\rho_{\rm gs}(\underline{r})}\right\} - 1\right]\\ &-\frac{1}{2}\int \mathrm{d}\underline{r}\,\mathrm{d}\underline{r}'\,c(\underline{r}-\underline{r}')[\rho(\underline{r},t)-\rho_{\rm gs}(\underline{r})][\rho(\underline{r}',t)-\rho_{\rm gs}(\underline{r}')]\\ &+\beta\int \mathrm{d}\underline{r} V_{uv}^{\rm ex}(\underline{r}-\underline{R})[\rho(\underline{r},t)-\rho_{\rm gs}(\underline{r})],\end{aligned} \tag{5}$$

where $\rho(\underline{r},t) = \rho_{\rm gs}(\underline{r}) + \delta\rho(\underline{r},t)$, $\delta\rho(\underline{r},t)$ being the fluctuation from the position and time-dependent density of the solvent in the presence of the solute in its ground state, $\rho_{\rm gs}(\underline{r},t)$.

Considering only the linear order terms in $\delta\rho(\underline{r},t)$ in eq. (5), we obtain the following expression for the current term:

$$\begin{aligned}\underline{j} = -D\Bigg[&\underline{\nabla}\delta\rho(\underline{r},t) - \frac{1}{\rho_0}\delta\rho(\underline{r},t)\underline{\nabla}\delta\rho_{\rm gs}(\underline{r})\\ &-\rho_0\underline{\nabla}\int \mathrm{d}\underline{r}'\,c(\underline{r}-\underline{r}')\delta\rho(\underline{r}',t)\\ &-\delta\rho_{\rm gs}(\underline{r})\underline{\nabla}\int \mathrm{d}\underline{r}'\,c(\underline{r}-\underline{r}')\delta\rho(\underline{r}',t) + \beta\delta\rho(\underline{r},t)\underline{\nabla}V_{uv}^{\rm ex}(\underline{r})\Bigg].\end{aligned} \tag{6}$$

Substituting eq. (5) in eq. (4) and Fourier transforming both over space and time (details in Appendix B), we obtain

$$\begin{aligned}\frac{\omega\sigma^2}{D}\delta\rho(\underline{q},\omega) = &-q^2[1-\rho_0 c(\underline{q})]\delta\rho(\underline{q},\omega)\\ &+\frac{1}{\rho_0}\sum_{\underline{k}}\underline{q}\cdot(\underline{q}-\underline{k})\delta\rho_{\rm gs}(\underline{q}-\underline{k})\delta\rho(\underline{k},\omega)\\ &+\sum_{\underline{k}}\underline{k}\cdot\underline{q}c(\underline{k})\delta\rho_{\rm gs}(\underline{q}-\underline{k})\delta\rho(\underline{k},\omega)\\ &-\beta\sum_{\underline{k}}\underline{q}\cdot(\underline{q}-\underline{k})V_{uv}^{\rm ex}(\underline{q}-\underline{k})\delta\rho(\underline{k},\omega),\end{aligned}\tag{7}$$

where $\delta\rho(\underline{r},t)=\sum_{\underline{q}}\delta\rho(\underline{q},\omega)\exp(\omega t+i\underline{q}\cdot\underline{r})$, ω being the frequency. Note that in eq. (7), a density mode with momentum $\underline{q}$ is linearly coupled to another mode with momentum $\underline{k}$. Due to symmetry, the term $\sum_{\underline{k}}\underline{k}\cdot\underline{q}\delta\rho_{\rm gs}(\underline{q}-\underline{k})c(\underline{k})\delta\rho(\underline{k},\omega)$ vanishes on integration over the angle between $\underline{k}$ and $\underline{q}$.

Equation (7) can also be written as the following closed form:

$$\omega\sigma^2 D^{-1}\delta\rho(\underline{q},\omega)=\sum_{\underline{k}}\Omega_{\underline{q},\underline{q}-\underline{k}}\delta\rho(\underline{k},\omega),\tag{8}$$

where $\Omega_{\underline{q},\underline{q}-\underline{k}}=-q^2[1-\rho_0 c(\underline{q})]+[(1/\rho_0)\delta\rho_{\rm gs}(\underline{q}-\underline{k})-V_{uv}^{\rm ex}(\underline{q}-\underline{k})]\underline{q}\cdot(\underline{q}-\underline{k})$ represents the stability matrix. Here, the first term $-q^2[1-\rho_0 c(\underline{q})]\delta\rho(\underline{q},\omega)$ originates from the pair correlation between the solvent molecules and hence, is related to the static structure factor of the solvent. The scattering by the solute–solvent interaction of the modes with wave-vector $\underline{q}$ and $\underline{k}$ gives rise to the second term. As expected, this term also derives contributions from the solvent density distribution in the presence of the solute in its ground state.

The positive eigenvalues (in frequency) of stability matrix in eq. (8) indicate the growing modes in the system and the maximum positive frequency will be the dominant mode [17]. Here we are looking for the most unstable mode of the solvent density such that we can identify the driving force for the solvent rearrangement in the excited state of the solute and, as a result, we can infer about the time scale for the solvation.

3. Non-polar solvation

We now apply the theory developed in §2 to systems governed by the non-polar interactions. Let us consider that the solvent molecules are interacting via the Lennard–Jones potential [23] $V_{\rm LJ}(r)=4\varepsilon[(\sigma/r)^{12}-(\sigma/r)^6]$ with ε being the ground state solvent–solvent interaction strength and σ the diameter of the solvent molecule. We further assume that the interaction between a solute at $\underline{R}$ in its ground state and a solvent at $\underline{r}$ is given as $V_{uv}^{\rm gs}(|\underline{r}-\underline{R}|)=4\varepsilon[(\sigma/|\underline{r}-\underline{R}|)^{12}-(\sigma/|\underline{r}-\underline{R}|)^6]$. Note here that the solute molecule in its ground state is simply one of the solvent molecules. However, the interaction between the excited solute and solvent

molecules differs only in the interaction strength and is given as $V_{uv}^{\rm ex}(|\underline{r}-\underline{R}|) = fV_{uv}^{\rm gs}(|\underline{r}-\underline{R}|)$ where f is the ratio of the interaction strengths between the excited and ground states of the solute with the solvent molecules.

For the direct correlation function $c(r)$, we consider the Percus–Yevick (PY) closure for the short-ranged repulsion [23]. The mean field (MF) approximation provides additional contribution to the pair correlation due to the long-ranged attractive interaction present in the system [23]. Therefore, the total pair correlation is approximated [23] as $c(r) = c_{\rm PY}(r) + c_{\rm MF}(r)$ where $c_{\rm MF}(r) = -\beta V(r), V(r)$ being the long-ranged attractive part of the solvent–solvent interaction potential, $V_{\rm LJ}(r)$.

We can describe the effects of the solute–solvent interactions as a scattering process [17] where a solvent density mode with momentum $\underline{q}$ is scattered to another density mode of momentum $\underline{k}$ at an angle χ, with transfer of momentum $p = |\underline{q}-\underline{k}|$. From eq. (3) we note that the scattering amplitude is governed by $V_{\rm gs}(p)$ where the maximum contribution arises from the low momentum transfer processes. This corresponds to the elastic scattering process where the scattered density mode is just rotated by the angle χ due to the interaction [17]. Note here that the elastic scattering term will contribute to the diagonal element of the stability matrix given in eq. (8). Now for low momentum transfer process, we can expand the interaction potential as [17] $V_{\rm gs}(p) = V_{\rm gs}^{(0)} - \frac{1}{2}p^2 V_{\rm gs}^{(2)}$ where $V_{\rm gs}^{(0)} = 4\pi \int {\rm d}r\, r^2 V_{\rm gs}(r)$ and $V_{\rm gs}^{(2)} = (4\pi/3)\int {\rm d}r\, r^4 V_{\rm gs}(r)$. Subsequently, a straightforward algebra (details are in Appendix C) leads to the expressions $V_{\rm gs}^{(0)} = -(16/3)\pi\varepsilon = V_{\rm gs}^{(2)}$ and $V_{\rm ex}^{(0)} = fV_{\rm gs}^{(0)} = -(16/3)\pi\varepsilon f = fV_{\rm gs}^{(2)}$.

3.1 *Diagonal element of the stability matrix in the long wavelength limit: Effects of compressibility*

As the compressibility of the system is associated with the long wavelength mode of the solvent density fluctuation, we consider the $q\sigma \sim 0$ limit of the diagonal element of the stability matrix given by eq. (8). In this limit, we can write $c(q)$ as

$$c(q) = C_0 - \frac{1}{2}q^2 C_2,$$

where

$$C_0 = 4\pi \int {\rm d}r\, r^2 c(r) \quad \text{and} \quad C_2 = \frac{4\pi}{3}\int {\rm d}r\, r^4 c(r).$$

Thus

$$C_0 = -\frac{1}{3}(4+\eta)\pi\lambda_1 - 6\pi\eta\lambda_2 + \frac{16}{3}\pi\varepsilon$$

and

$$C_2 = -\frac{\pi\lambda_1}{3}\left(\frac{4}{5}+\frac{1}{4}\eta\right) - \frac{4\pi}{3}\eta\lambda_2 + \frac{16}{3}\pi\varepsilon$$

where η is the packing fraction ($=(\pi/6)\rho^*$), and λ_1 and λ_2 are the constants as described in the PY closure relations [23]. The derivation of these terms is

given in Appendix C. Therefore, the contribution form the static solvent structure ('structural term') in the long wavelength limit ($q\sigma \sim 0$) is $A_{\rm st}^{(0)}q^2 + B_{\rm st}^{(0)}q^4$ where $A_{\rm st}^{(0)} = [\rho_0 C_0 - 1]$ and $B_{\rm st}^{(0)} = -\frac{1}{2}\rho_0 C_2$. The diagonal contribution from the scattering term is $A_{\rm sc}^{(0)}q^2 + B_{\rm sc}^{(0)}q^4$ where

$$A_{\rm sc}^{(0)} = -V_{\rm gs}^{(0)}\left[\frac{1}{1-\rho_0 C_0} + f\right]$$

and

$$B_{\rm sc}^{(0)} = \frac{4}{3}V_{\rm gs}^{(2)}\left[\frac{1}{1-\rho_0 C_0} + \frac{\rho_0 C_2}{(1-\rho_0 C_0)^2} + f\right].$$

Hence, the total diagonal term in the stability matrix in the $q\sigma \sim 0$ limit is $(A_{\rm G}q^2 + B_{\rm G}q^4)$ where $A_{\rm G} = A_{\rm st}^{(0)} + A_{\rm sc}^{(0)}$ and $B_{\rm G} = B_{\rm st}^{(0)} + B_{\rm sc}^{(0)}$ (for details see Appendix D).

3.2 *The diagonal term of the stability matrix around the ordering wave-vector: Effects of the ordering wave-vector (nearest-neighbour) modes*

At ordering wave-vector mode (that is, $q\sigma = q_0 \approx 2\pi$), the solvent static structure factor $S(q\sigma)$ possesses a sharp peak. Around q_0, the contribution from the structural term to the diagonal element is $A_{\rm st}(q\sigma)q^2$ where $A_{\rm st}(q\sigma) = -[1-\rho_0 c(q\sigma)]$. The contribution to the diagonal element from the elastic scattering is $A_{\rm sc}^{(2\pi)}q^2 + B_{\rm sc}^{(2\pi)}q^4$ where

$$A_{\rm sc}^{(2\pi)} = -\frac{1}{8\pi^3}V_{\rm gs}^{(0)}\left[\frac{1}{1-\rho_0 C_0} + f\right]$$

and

$$B_{\rm sc}^{(2\pi)} = \frac{1}{24\pi^5}V_{\rm gs}^{(2)}\left[\frac{1}{1-\rho_0 C_0} + f\right].$$

Therefore, the total diagonal contribution around q_0 is $A_{\rm L}q^2 + B_{\rm L}q^4$ where $A_{\rm L} = A_{\rm st}(q\sigma) + A_{\rm sc}^{(2\pi)}$ and $B_{\rm L} = B_{\rm sc}^{(2\pi)}$. The detailed derivation of these terms is provided in Appendix E.

3.3 *Off-diagonal elements: Effects of coupling between the solvent structure and excited state solute–solvent interaction at $q\sigma \sim 2\pi$*

In a normal liquid, both the compressibility and the structure factor of the solvent are expected to play significant roles in determining the instability of the solvent density modes, particularly when the system is governed by the non-polar interactions. In the present theory these quantities affect the instability via coupling with the ground state solute–solvent interaction ($V_{uv}^{\rm gs}$). However, the coupling of the excited state solute–solvent interaction ($V_{uv}^{\rm ex}$) with the solvent correlations at

the nearest-neighbour length scales in the presence of the ground state interaction may have non-trivial effects on the instability. Here we derive the analytical forms for the off-diagonal element obtained after considering the above coupling and consequently present the full stability matrix with all the elements shown explicitly. Assuming solvent static structure factor remains the same in the presence of the solute [17], the contribution due to the scattering in the presence of the ground state solute–solvent interaction can be given as

$$\frac{1}{\rho_0} 2\pi q q_0 \delta\rho_{\rm gs}(q_0) \int_0^1 {\rm d}(\cos\chi)\cos\chi = -\frac{1}{2} 2\pi q q_0 S(q_0) V_{\rm gs}(q_0).$$

Similarly, the scattering term due to the excited state solute–solvent interaction is

$$2\pi q q_0 f V_{\rm gs}(q_0) \int_0^1 {\rm d}(\cos\chi)\cos\chi = \frac{1}{2} 2\pi q q_0 f V_{\rm gs}(q_0).$$

The total off-diagonal term therefore becomes as follows:

$$\frac{1}{2\pi}[-\pi q q_0 S(q_0) V_{\rm gs}(q_0) - \pi q q_0 f V_{\rm gs}(q_0)] = -\frac{1}{2} q q_0 [S(q_0) + f] V_{\rm gs}(q_0), \quad (9)$$

where $1/2\pi$ arises due to the geometrical phase factor of the relative orientations of the incident and the scattered wave vectors.

Considering all the diagonal terms (§3.1 and 3.2) and off-diagonal terms in eq. (9), we now write the full stability matrix $\Omega_{q,Q}$ as follows:

$$\Omega_{q,Q} = \begin{bmatrix} A_{\rm G} q^2 + B_{\rm G} q^4 & -\frac{1}{2} q Q [S(q_0) + f] V_{\rm gs}(q_0) \\ \frac{1}{2} q Q [S(q_0) + f] V_{\rm gs}(q_0) & A_{\rm L} Q^2 + B_{\rm L} Q^4 \end{bmatrix}, \quad (10)$$

where q is the mode corresponding to the compressibility and Q is the mode around q_0.

4. Results and discussion

In our calculation, we take $\sigma \sim 10^{-8}$ cm and $D \sim 10^{-5}$ cm^2 s^{-1}. The energy is scaled by $k_{\rm B}T$, length by σ and time by $(\sigma^2/D) \approx 1$ ps. The calculation is done at $T = 2T_{\rm c}$, $T_{\rm c}$ being the critical temperature of the system. Dimensionless quantities are represented using asterisk as superscript.

4.1 *Long wavelength limit* ($q\sigma \sim 0$)

Retaining only the $q\sigma \sim 0$ mode, eq. (10) can be expressed as $\omega^*(q^*) = A_{\rm G} q^{*2} + B_{\rm G} q^{*4}$. For the maximum positive eigenvalue of the stability matrix $({\rm d}\omega^*(q^*)/{\rm d}q^*) = 0$. Therefore,

$$\omega^*_{\rm max} = -\frac{1}{4}\frac{A_{\rm G}^2}{B_{\rm G}} \quad \text{at} \quad q^*_{\rm max} = -\frac{1}{2}\frac{A_{\rm G}}{B_{\rm G}}.$$

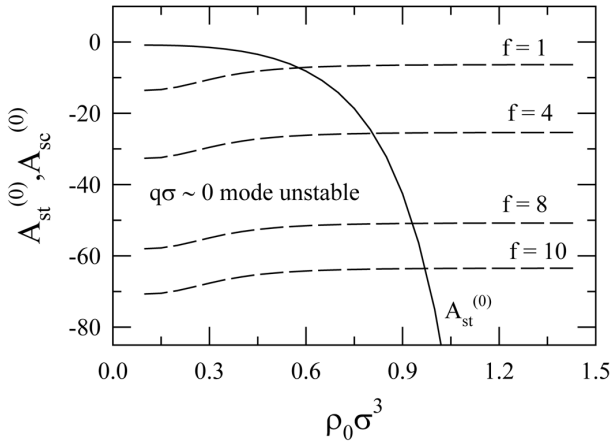

Figure 1. Plot of the structural ($A_{\rm st}$) and the scattering terms ($A_{\rm sc}$) in the $q\sigma \sim 0$ limit. Note here that the solid line represents $A_{\rm st}$ while the broken lines represent $A_{\rm sc}$ at different values of f which is the ratio between the solute–solvent interaction strengths between the excited and ground states. That is, $f = \varepsilon_{uv}^{\rm ex}/\varepsilon_{uv}^{\rm gs}$, u denoting the solute and v the solvent. Note the sharp decay of $A_{\rm st}$ with density and the very weak density dependence of $A_{\rm sc}$. For further details, see text.

The corresponding time scale is $\tau^* = 1/\omega_{\rm max}^*$. The discussions in §3.1 indicate that $A_{\rm G}$ derives contributions from two competing terms, $A_{\rm st}^{(0)}$ and $A_{\rm sc}^{(0)}$, which are coming respectively from the structural correlation and scattering due to the solute–solvent interactions. Figure 1 depicts the competition where density dependence of these two terms are shown at several values of the ratio between solute–solvent interactions at the excited and the ground states. In figure 1, the solid line corresponds to the structural term $A_{\rm st}^{(0)}$ and the dashed lines describe the behaviour of the scattering term $A_{\rm sc}^{(0)}$ for different f. It is interesting to note that while $A_{\rm st}^{(0)}$ decays relatively sharply with density, $A_{\rm sc}^{(0)}$ remains almost insensitive to the density for the entire range. The left-hand side of the intersection point for a given f corresponds to the region of instability for $q\sigma \sim 0$ mode and the right-hand side corresponds to the stable ground state with respect to the density perturbation with $q\sigma \sim 0$ mode. This means that on the right-hand side of this intersecting line, the present theory does not predict any instability corresponding to $q\sigma \sim 0$. As the system becomes more incompressible with the increase in density, the long wavelength instability at a given f becomes more and more suppressed. With increase in f, there is a shift of the intersection point towards high density which implies that the long wavelength instability can be supported further by the solute–solvent interaction. Near the intersection point on the left half, τ^* can become very large. The origin of this long time scale is the competition between long wavelength compressibility of the system and the solute–solvent interaction-induced structure.

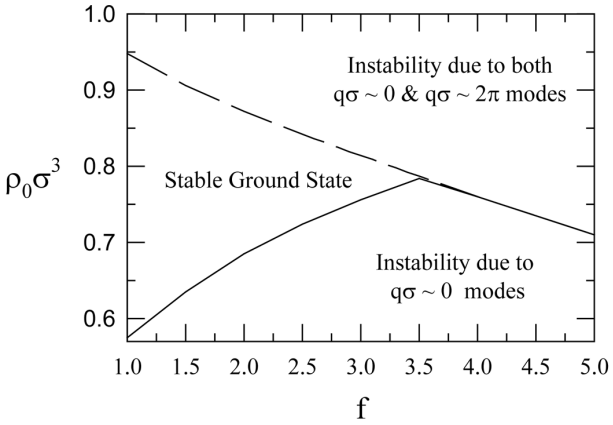

Figure 2. Instability diagram in the $\rho_0\sigma^3$ vs. f plane where $f = \varepsilon_{uv}^{\rm ex}/\varepsilon_{uv}^{\rm gs}$. The solid line represents the instability line for the compressible region where instability is supported only by the $q\sigma \sim 0$ mode. The dashed line depicts the instability line where instability is induced by both $q\sigma \sim 0$ and $q\sigma \sim 2\pi$ modes. The region on and above the broken lines are prone to instability by both the above modes, whereas the triangle-shaped area bound by the broken and solid line is completely devoid of any instability. The low density compressible region which is characterized by the instability due to $q\sigma \sim 0$ mode is also shown.

4.2 *Instability diagram*

We include the effects of the $q\sigma \sim 2\pi$ mode also and set out for constructing a diagram that would describe the presence of the instability for a given value of f at a particular density. After diagonalizing the stability matrix given in eq. (10), the maximum positive eigenvalues for several densities as a function of the ratio between the solute–solvent interaction strength (f) are calculated. The densities corresponding to the maximum positive eigenvalues are shown as a function of f in figure 2. Interestingly, figure 2 depicts three regions in the $\rho_0\sigma^3$ vs. f plane, showing instability due to the modes investigated. Here, the solid line corresponds to the limit of instability for compressible situation below which the system is unstable for $q\sigma \sim 0$ mode only. The dashed line corresponds to the limit of instability for both the modes. Above the dashed line the system is unstable for both $q\sigma \sim 0$ and $q\sigma \sim 2\pi$ modes. In between these two regions, there is no instability for both the modes, namely, the ground state of the system is stable with respect to the non-equilibrium density perturbation.

The topology of the instability diagram is quite distinct for low and high values of f. Let us consider $f = 2$. Here, for $\rho_0\sigma^3 < 0.67$, there is only one long time scale due to $q\sigma \sim 0$ mode, while we get time scales corresponding to both $q\sigma \sim 0$ and $q\sigma \sim 2\pi$ modes for $\rho_0\sigma^3 > 0.97$. In the intermediate density range, we obtain stable ground state. However, at $f = 4$, only one long time scale is obtained in the low density region ($\rho_0\sigma^3 < 0.75$) due to the $q\sigma \sim 0$ mode, while two long time scales are obtained at higher densities due to both $q\sigma \sim 0$ and $q\sigma \sim 2\pi$ modes. Let

us now consider the topology at constant values of densities for different f. One can distinguish between four different possibilities. For instance, at $\rho_0\sigma^3 \approx 1.0$, there are two long time scales for all values of f. At $\rho_0\sigma^3 = 0.8$, the ground state is stable for $f < 3.2$. One encounters two long time scales for larger f. At $\rho_0\sigma^3 = 0.7$, the ground state is stable up to $f = 2.2$. Then there is one long time scale due to $q\sigma \sim 0$ mode up to $f = 4.8$ and two long time scales for larger f. For $\rho_0\sigma^3 = 0.5$, there is only one long time scale due to $q\sigma \sim 0$ mode for all f.

The region where both the modes are unstable is the most interesting region as this region produces time scales, one in the range of 1–2 ps and the other in the range of $\geq$10 ps for $f = 4$ as reported earlier [17]. Note also that both the values of f ($f = 4$) and density for which these two time scales are predicted are very close to the solute–solvent systems for which the experiments have reported multiple time scales in the long time decay of solvent response function [13]. Even though the present calculation is done for size ratio of unity, the time scales are expected to be similar for different solute–solvent size ratios as well. Indeed, the experimental studies have revealed that the long time constant changes approximately by 20% on increasing the solute size by a factor of 5, while the fast time constant remains insensitive to such a change [4]. In the theory presented here the longer time scale originates from compressibility of the system, whereas the shorter time scale comes from the nearest-neighbour arrangement of the solvent molecules.

It is interesting to compare the instability diagram with the results in figure 1. For lower f, there exists the region where the ground state is stable, in agreement with figure 1. However, at still higher density, there is an unstable region unlike figure 1. At very high density the solvent structure affects the instability of $q\sigma \sim 2\pi$ mode. Due to its coupling to the compressibility mode, it influences the instability of the compressibility mode as well. We obtain multiple long time scales over this region.

5. Conclusion

The salient features of the work presented here are as follows. The theory suggests that for non-polar solvation dynamics, the experimentally observed multiple time scales associated with the long time decay of the solvent response function may originate from the compressibility and the nearest-neighbour arrangement of the solvent around the solute. While the compressibility is responsible for the longer time scales, the nearest-neighbour arrangement controls the relatively shorter time constant via the peak of the static structure factor of the solvent. However, the effects of these solvent properties on time scales are mediated via the solute–solvent interactions both at the ground and the excited states of the solute. Moreover, the coupling of the ordering wave-vector mode with the ground and excited state solute–solvent interactions leads to the modification of both the time scales. Note that earlier theories did not incorporate such effects while predicting the solvation energy relaxation in terms of either the liquid dynamic structure factor [12] or employing the full solution of NLHE [15]. As the present theory systematically incorporates the competition between the long wavelength fluctuations (related to compressibility) and the nearest-neighbour arrangement ($q\sigma \sim 2\pi$ mode), this ap-

proach may generate molecular level understanding of solvation time scales observed experimentally for systems near the critical temperature [16].

The instability diagram (figure 2) indicates a significant area in the $\rho_0\sigma^3$ vs. f plane where no instability is predicted. This means that for these values of density interactions would not produce enough perturbation in the liquid structure to enable the solvation of the excited solute. While this may be a possibility for a vitrified system at a very low temperature, this certainly is not real for the thermodynamic condition ($T = 2T_c$) considered here. This artifact can be removed by explicitly considering the solute–solvent size ratio, which is missing in the theory presented here. Also, systematic incorporation of the solvent inertial motion is likely to modify the instability diagram in a significant manner. However, the 'no instability' zone will exist because linear stability analysis approach is insufficient for situations where non-linear effects (that is inclusion of higher-order terms in density fluctuation) dominate. Another lacuna of the present theory is its inability to predict the full decay of the solvent response function, $S(t)$, as this requires the calculation of the decay amplitudes. Consideration of the non-linear terms may be helpful for this purpose.

The present theory can be extended to incorporate the solvent inertial motion for non-polar systems and also for the systems where dipolar or higher-order polar interactions drive the solvation process. For polar interactions, one needs to consider the angle dependence which would make the entire calculation very non-trivial and computationally involved. The present theory can also be employed for ionic solutions, ionic liquids and liquids under stress. Some of the works reported above are already in progress [24].

Appendix A: Derivation of the solvent inhomogeneity in the presence of the solute in its ground state

We have $\rho(\underline{r}) = \rho_0 + \delta\rho_{\rm gs}(\underline{r})$. Therefore,

$$\ln\left\{\frac{\rho(\underline{r})}{\rho_0}\right\} = \ln\left\{1 + \frac{\delta\rho_{\rm gs}(\underline{r})}{\rho_0}\right\} = \frac{\delta\rho_{\rm gs}(\underline{r})}{\rho_0} - \frac{1}{2}\left\{\frac{\delta\rho_{\rm gs}(\underline{r})}{\rho_0}\right\}^2$$

(neglecting the higher-order terms as $\delta\rho_{\rm gs}(r) \ll \rho_0$) and

$$\rho(\underline{r})\ln\left(\frac{\rho(\underline{r})}{\rho_0}\right) = \delta\rho_{\rm gs}(\underline{r}) + \frac{1}{2}\frac{\{\delta\rho_{\rm gs}(\underline{r})\}^2}{\rho_0}$$

(considering up to quadratic terms). Putting this in eq. (1) we get

$$\begin{aligned}\beta F^{\rm gs}[\rho(\underline{r})] = &\int \mathrm{d}\underline{r}\left[\delta\rho_{\rm gs}(\underline{r}) + \frac{1}{2}\frac{\{\delta\rho_{\rm gs}(\underline{r})\}^2}{\rho_0}\right] \\ &-\frac{1}{2}\int \mathrm{d}\underline{r}\,\mathrm{d}\underline{r}'\,c(\underline{r}-\underline{r}')\delta\rho_{\rm gs}(\underline{r})\delta\rho_{\rm gs}(\underline{r}') \\ &+\int \mathrm{d}\underline{r}[\rho_0 + \delta\rho_{\rm gs}(\underline{r})][\beta V_{uv}^{\rm gs}(\underline{r}-\underline{R}) - 1]. \qquad \text{(A.1)}\end{aligned}$$

At equilibrium, $(\delta\beta F^{\rm gs}[\rho(\underline{r})]/\delta\rho_{\rm gs}(\underline{r})) = 0$ where $\beta F^{\rm gs}[\rho(\underline{r})]$ is given by eq. (A.1). Or,

$$\frac{1}{\rho_0}\delta\rho_{\rm gs}(\underline{r}) - \int \mathrm{d}\underline{r}'\, c(\underline{r}-\underline{r}')\delta\rho_{\rm gs}(\underline{r}') + \beta V_{uv}^{\rm gs}(\underline{r}-\underline{R}) = 0. \tag{A.2}$$

Using the following definitions of the Fourier transform (FT) $f(\underline{r}) = \frac{1}{(2\pi)^3}\int \mathrm{d}\underline{k}\, f(\underline{k})\, \mathrm{e}^{i\underline{k}\cdot\underline{r}}$ and $f(\underline{k}) = \int \mathrm{d}\underline{r} f(\underline{r})\mathrm{e}^{-i\underline{k}\cdot\underline{r}}$ and setting $\underline{R} = 0$, from eq. (A.2) we obtain $\frac{1}{\rho_0}\delta\rho_{\rm gs}(\underline{q}) = c(\underline{q})\delta\rho_{\rm gs}(\underline{q}) - \beta V_{uv}^{\rm gs}(\underline{q})$, which, on rearrangement, provides

$$\delta\rho_{\rm gs}(\underline{q}) = \frac{-\beta\rho_0 V_{uv}^{\rm gs}(\underline{q})}{1-\rho_0 c(\underline{q})}, \tag{A.3}$$

where eq. (A.3) gives the ground state inhomogeneity in the system due to insertion of the solute.

Appendix B: Derivation of the stability matrix $\boldsymbol{\Omega_{\underline{q},\underline{q}-\underline{k}}}$

We have, $\rho(\underline{r},t) = \rho_{\rm gs}(\underline{r}) + \delta\rho(\underline{r},t)$ and $\rho_{\rm gs}(\underline{r}) = \rho_0 + \delta\rho_{\rm gs}(\underline{r})$. Considering only up to quadratic terms, we can write

$$\ln\left[\frac{\rho(\underline{r},t)}{\rho_{\rm gs}(\underline{r})}\right] = \frac{\delta\rho(\underline{r},t)}{\rho_0+\delta\rho_{\rm gs}(\underline{r})} - \frac{1}{2}\left[\frac{\delta\rho(\underline{r},t)}{\rho_0+\delta\rho_{\rm gs}(\underline{r})}\right]^2$$

and

$$\begin{aligned}
\rho(\underline{r},t)\ln\left[\frac{\rho(\underline{r},t)}{\rho_{\rm gs}(\underline{r})}\right] &= \delta\rho(\underline{r},t) - \frac{1}{2}\frac{[\delta\rho(\underline{r},t)]^2}{\rho_0+\delta\rho_{\rm gs}(\underline{r})} + \frac{[\delta\rho(\underline{r},t)]^2}{\rho_0+\delta\rho_{\rm gs}(\underline{r})} \\
&= \delta\rho(\underline{r},t) + \frac{1}{2\rho_0}\frac{[\delta\rho(\underline{r},t)]^2}{\left[1+\frac{\delta\rho_{\rm gs}(\underline{r})}{\rho_0}\right]} \\
&= \delta\rho(\underline{r},t) + \frac{1}{2\rho_0}[\delta\rho(\underline{r},t)]^2\left[1+\frac{\delta\rho_{\rm gs}\,(\underline{r})}{\rho_0}\right]^{-1} \\
&= \delta\rho(\underline{r},t) + \frac{1}{2\rho_0}[\delta\rho(\underline{r},t)]^2 - \frac{1}{2\rho_0^2}\delta\rho_{\rm gs}(\underline{r})[\delta\rho(\underline{r},t)]^2.
\end{aligned} \tag{B.1}$$

Putting eq. (B.1) in free energy expression for the excited state we obtain

$$\begin{aligned}
\beta F^{\rm ex}[\rho(\underline{r},t)] = &\int \mathrm{d}\underline{r}\left[\delta\rho(\underline{r},t) + \frac{1}{2\rho_0}\{\delta\rho(\underline{r},t)\}^2 - \frac{1}{2\rho_0^2}\delta\rho_{\rm gs}(\underline{r})\{\delta\rho(\underline{r},t)\}^2\right] \\
&- \int \mathrm{d}\underline{r}[\rho_0 + \delta\rho_{\rm gs}(\underline{r}) + \delta\rho(\underline{r},t)] \\
&- \frac{1}{2}\int \mathrm{d}\underline{r}\,\mathrm{d}\underline{r}'\, c(\underline{r}-\underline{r}')\delta\rho(\underline{r},t)\delta\rho(\underline{r}',t) \\
&+ \beta\int \mathrm{d}\underline{r}\, V_{uv}^{\rm ex}(\underline{r}-\underline{R})\delta\rho(\underline{r},t).
\end{aligned} \tag{B.2}$$

Therefore,

$$\beta\mu = \frac{\delta\beta F^{\rm ex}[\rho(\underline{r},t)]}{\delta\rho(\underline{r},t)}.$$

Using eq. (B.2) we get

$$\beta\mu = \frac{1}{\rho_0}\delta\rho(\underline{r},t) - \frac{1}{\rho_0^2}\delta\rho_{\rm gs}(\underline{r})\delta\rho(\underline{r},t) - \int \mathrm{d}\underline{r}'\, c(\underline{r}-\underline{r}')\delta\rho(\underline{r}',t) + \beta V_{uv}^{\rm ex}(\underline{r}-\underline{R}),$$

or,

$$\begin{aligned}\beta\mu = {} & \frac{1}{\rho_0}\delta\rho(\underline{r},t) - \frac{1}{\rho_0^2}\delta\rho_{\rm gs}(\underline{r})\delta\rho(\underline{r},t) \\ & - \int \mathrm{d}\underline{r}'\, c(\underline{r}-\underline{r}')\delta\rho(\underline{r}',t) + \beta V_{uv}^{\rm ex}(\underline{r}) \quad (\text{setting } \underline{R}=0). \end{aligned} \tag{B.3}$$

In the over-damped limit, velocity

$$\begin{aligned}\underline{v} &= -D\underline{\nabla}(\beta\mu) \\ &= -D\bigg[\frac{1}{\rho_0}\underline{\nabla}\delta\rho(\underline{r},t) - \frac{1}{\rho_0^2}\delta\rho_{\rm gs}(\underline{r})\underline{\nabla}\delta\rho(\underline{r},t) \\ &\quad -\frac{1}{\rho_0^2}\delta\rho(\underline{r},t)\underline{\nabla}\delta\rho_{\rm gs}(\underline{r}) \quad (\text{using (B.3)}) \\ &\quad -\underline{\nabla}\int \mathrm{d}\underline{r}'c(\underline{r}-\underline{r}')\delta\rho(\underline{r}',t) + \beta\underline{\nabla}V_{uv}^{\rm ex}(\underline{r})\bigg]. \end{aligned} \tag{B.4}$$

Since $\underline{j} = \rho(\underline{r},t)\underline{v}$, we can write using eq. (B.4)

$$\begin{aligned}\underline{j} = {} & -D[\rho_0 + \delta\rho_{\rm gs}(\underline{r}) + \delta\rho(\underline{r},t)]\bigg[\frac{1}{\rho_0}\underline{\nabla}\delta\rho(\underline{r},t) \\ & -\frac{1}{\rho_0^2}\delta\rho_{\rm gs}(\underline{r})\underline{\nabla}\delta\rho(\underline{r},t) - \frac{1}{\rho_0^2}\delta\rho(\underline{r},t)\underline{\nabla}\delta\rho_{\rm gs}(\underline{r}) \\ & -\underline{\nabla}\int \mathrm{d}\underline{r}'\, c(\underline{r}-\underline{r}')\delta\rho(\underline{r}',t) + \beta\nabla V_{uv}^{\rm ex}(\underline{r})\bigg]. \end{aligned} \tag{B.5}$$

Considering only the linear order terms for $\delta\rho_{\rm gs}(\underline{r})$ and $\delta\rho(\underline{r},t)$ we get from eq. (B.5),

$$\begin{aligned}j = {} & -D\bigg[\underline{\nabla}\delta\rho(\underline{r},t) - \frac{1}{\rho_0}\delta\rho(\underline{r},t)\underline{\nabla}\delta\rho_{\rm gs}(\underline{r}) \\ & -\rho_0\underline{\nabla}\int \mathrm{d}\underline{r}'\, c(\underline{r}-\underline{r}')\delta\rho(\underline{r}',t) + \beta\rho_0\underline{\nabla}V_{uv}^{\rm ex}(\underline{r}) \\ & -\delta\rho_{\rm gs}(\underline{r})\underline{\nabla}\int \mathrm{d}\underline{r}'c(\underline{r}-\underline{r}')\delta\rho(\underline{r}',t) \\ & +\beta\delta\rho_{\rm gs}(\underline{r})\underline{\nabla}V_{uv}^{\rm ex}(\underline{r}) + \beta\delta\rho(\underline{r},t)\underline{\nabla}V_{uv}^{\rm ex}(\underline{r})\bigg]. \end{aligned} \tag{B.6}$$

As we are interested in the time-dependent inhomogeneity of the excited system, we ignore the time-independent parts in eq. (B.6). Thus we get

$$\begin{aligned}\underline{j} = -D\Bigg[&\underline{\nabla}\delta\rho(\underline{r},t) - \frac{1}{\rho_0}\delta\rho(\underline{r},t)\underline{\nabla}\delta\rho_{\rm gs}(\underline{r}) \\ &-\rho_0\underline{\nabla}\int \mathrm{d}\underline{r}'\, c(\underline{r}-\underline{r}')\delta\rho(\underline{r}',t) \\ &-\delta\rho_{\rm gs}(\underline{r})\underline{\nabla}\int \mathrm{d}\underline{r}' c(\underline{r}-\underline{r}')\delta\rho(\underline{r}',t) + \beta\delta\rho(\underline{r},t)\underline{\nabla}V_{uv}^{\rm ex}(\underline{r})\Bigg]. \end{aligned} \tag{B.7}$$

Therefore, using eq. (B.7) we have

$$\begin{aligned}\underline{\nabla}\underline{j} = -D\Bigg[&\nabla^2\delta\rho(\underline{r},t) - \frac{1}{\rho_0}\underline{\nabla}\delta\rho(\underline{r},t)\underline{\nabla}\delta\rho_{\rm gs}(\underline{r}) - \frac{1}{\rho_0}\delta\rho(\underline{r},t)\nabla^2\delta\rho_{\rm gs}(\underline{r}) \\ &-\rho_0\nabla^2\int \mathrm{d}\underline{r}'\, c(\underline{r}-\underline{r}')\delta\rho(\underline{r}',t) - \underline{\nabla}\delta\rho_{\rm gs}(\underline{r})\underline{\nabla}\int \mathrm{d}\underline{r}'\, c(\underline{r}-\underline{r}')\delta\rho(\underline{r}',t) \\ &-\delta\rho_{\rm gs}(\underline{r})\nabla^2\int \mathrm{d}\underline{r}'\, c(\underline{r}-\underline{r}')\delta\rho(\underline{r}',t) + \beta\underline{\nabla}\delta\rho(\underline{r},t)\underline{\nabla}V_{uv}^{\rm ex}(\underline{r}) \\ &+\beta\delta\rho(\underline{r},t)\nabla^2 V_{uv}^{\rm ex}(\underline{r})\Bigg]. \end{aligned} \tag{B.8}$$

Putting eq. (B.8) in eq. (4) and rearranging we get

$$\begin{aligned}\partial_t\rho(\underline{r},t) = D\Bigg[&\nabla^2\delta\rho(\underline{r},t) - \frac{1}{\rho_0}\underline{\nabla}\delta\rho(\underline{r},t)\underline{\nabla}\delta\rho_{\rm gs}(\underline{r}) \\ &-\frac{1}{\rho_0}\delta\rho(\underline{r},t)\nabla^2\delta\rho_{\rm gs}(\underline{r}) - \rho_0\nabla^2\int \mathrm{d}\underline{r}' c(\underline{r}-\underline{r}')\delta\rho(\underline{r}',t) \\ &-\underline{\nabla}\delta\rho_{\rm gs}(\underline{r})\underline{\nabla}\int \mathrm{d}\underline{r}'\, c(\underline{r}-\underline{r}')\delta\rho(\underline{r}',t) \\ &-\delta\rho_{\rm gs}(\underline{r})\nabla^2\int \mathrm{d}\underline{r}' c(\underline{r}-\underline{r}')\delta\rho(\underline{r}',t) \\ &+\beta\underline{\nabla}\delta\rho(\underline{r},t)\underline{\nabla}V_{uv}^{\rm ex}(\underline{r}) + \beta\delta\rho(\underline{r},t)\nabla^2 V_{uv}^{\rm ex}(\underline{r})\Bigg]. \end{aligned} \tag{B.9}$$

After Fourier transformation, eq. (B.9) becomes

$$\begin{aligned}\partial_t\rho(\underline{q},t) = D\Bigg[&-q^2\delta\rho(\underline{q},t) + \frac{1}{\rho_0(2\pi)^3}\int \mathrm{d}\underline{k}\,\underline{k}(\underline{q}-\underline{k})\delta\rho_{\rm gs}(\underline{q}-\underline{k})\delta\rho(\underline{k},t) \\ &+\frac{1}{\rho_0(2\pi)^3}\int \mathrm{d}\underline{k}\,(\underline{q}-\underline{k})^2\delta\rho_{\rm gs}(\underline{q}-\underline{k})\delta\rho(\underline{k},t) + \rho_0 q^2 c(\underline{q})\delta\rho(\underline{q},t) \\ &+\frac{1}{(2\pi)^3}\int \mathrm{d}\underline{k}\,\underline{k}(\underline{q}-\underline{k})\delta\rho_{\rm gs}(\underline{q}-\underline{k})c(\underline{k})\delta\rho(\underline{k},t) \\ &+\frac{1}{(2\pi)^3}\int \mathrm{d}\underline{k}k^2\delta\rho_{\rm gs}(\underline{q}-\underline{k})c(\underline{k})\delta\rho(\underline{k},t) \end{aligned}$$

$$-\frac{\beta}{(2\pi)^3}\int \mathrm{d}\underline{k}\,\underline{k}(\underline{q}-\underline{k})V_{uv}^{\mathrm{ex}}(\underline{q}-\underline{k})\delta\rho(\underline{k},t)$$
$$-\frac{\beta}{(2\pi)^3}\int \mathrm{d}\underline{k}(\underline{q}-\underline{k})^2V_{uv}^{\mathrm{ex}}(\underline{q}-\underline{k})\delta\rho(\underline{k},t)\Bigg].$$

The following expression for the Fourier transformed quantities are used in the above equation:

$$\text{FT of } \nabla^2\delta\rho(\underline{r},t) = -q^2\delta\rho(\underline{q},t),$$
$$\text{FT of } \frac{1}{\rho_0}\underline{\nabla}\delta\rho(\underline{r},t)\underline{\nabla}\delta\rho_{\mathrm{gs}}(\underline{r})$$
$$= -\frac{1}{\rho_0(2\pi)^3}\int \mathrm{d}\underline{k}\,\underline{k}(\underline{q}-\underline{k})\delta\rho_{\mathrm{gs}}(\underline{q}-\underline{k})\delta\rho(\underline{k},t),$$
$$\text{FT of } \frac{1}{\rho_0}\delta\rho(\underline{r},t)\nabla^2\delta\rho_{\mathrm{gs}}(\underline{r})$$
$$= -\frac{1}{\rho_0(2\pi)^3}\int \mathrm{d}\underline{k}\,(\underline{q}-\underline{k})^2\delta\rho_{\mathrm{gs}}(\underline{q}-\underline{k})\delta\rho(\underline{k},t),$$
$$\text{FT of } \rho_0\nabla^2\int \mathrm{d}\underline{r'}\,c(\underline{r}-\underline{r'})\delta\rho(\underline{r'},t) = -\rho_0q^2c(\underline{q})\delta\rho(\underline{q},t),$$
$$\text{FT of } \underline{\nabla}\delta\rho_{\mathrm{gs}}(\underline{r})\underline{\nabla}\int \mathrm{d}\underline{r'}\,c(\underline{r}-\underline{r'})\delta\rho(\underline{r'},t)$$
$$= -\frac{1}{(2\pi)^3}\int \mathrm{d}\underline{k}\,\underline{k}(\underline{q}-\underline{k})\delta\rho_{\mathrm{gs}}(\underline{q}-\underline{k})c(\underline{k})\delta\rho(\underline{k},t),$$
$$\text{FT of } \delta\rho_{\mathrm{gs}}(\underline{r})\nabla^2\int \mathrm{d}\underline{r'}c(\underline{r}-\underline{r'})\delta\rho(\underline{r'},t)$$
$$= -\frac{1}{(2\pi)^3}\int \mathrm{d}\underline{k}\,k^2\delta\rho_{\mathrm{gs}}(\underline{q}-\underline{k})c(\underline{k})\delta\rho(\underline{k},t),$$
$$\text{FT of } \beta\underline{\nabla}\delta\rho(\underline{r},t)\underline{\nabla}V_{uv}^{\mathrm{ex}}(\underline{r}) = -\frac{\beta}{(2\pi)^3}\int \mathrm{d}\underline{k}\,\underline{k}(\underline{q}-\underline{k})V_{uv}^{\mathrm{ex}}(\underline{q}-\underline{k})\delta\rho(\underline{k},t)$$

and

$$\text{FT of } \beta\delta\rho(\underline{r},t)\nabla^2V_{uv}^{\mathrm{ex}}(\underline{r}) = -\frac{\beta}{(2\pi)^3}\int \mathrm{d}\underline{k}\,(\underline{q}-\underline{k})^2V_{uv}^{\mathrm{ex}}(\underline{q}-\underline{k})\delta\rho(\underline{k},t).$$

Now we Fourier transform $\partial_t\rho(\underline{q},t)$ in order to obtain the following expression in the frequency (ω) plane:

$$\omega\sigma^2\delta\rho(\underline{q},\omega) = D\Bigg[-q^2\{1-\rho_0c(\underline{q})\}\delta\rho(\underline{q},\omega)$$
$$+\frac{1}{\rho_0(2\pi)^3}\int \mathrm{d}\underline{k}\underline{q}\cdot(\underline{q}-\underline{k})\delta\rho_{\mathrm{gs}}(\underline{q}-\underline{k})\delta\rho(\underline{k},\omega)$$
$$+\frac{1}{(2\pi)^3}\int \mathrm{d}\underline{k}\,\underline{k}\cdot\underline{q}c(\underline{k})\delta\rho_{\mathrm{gs}}(\underline{q}-\underline{k})\delta\rho(\underline{k},\omega)$$
$$-\frac{\beta}{(2\pi)^3}\int \mathrm{d}\underline{k}\underline{q}\cdot(\underline{q}-\underline{k})V_{uv}^{\mathrm{ex}}(\underline{q}-\underline{k})\delta\rho(\underline{k},\omega)\Bigg],$$

which gives

$$\omega\sigma^2 D^{-1}\delta\rho(\underline{q},\omega) = \sum_{\underline{k}} \Omega_{\underline{q},\underline{q}-\underline{k}}\delta\rho(\underline{k},\omega), \tag{B.10}$$

where $\Omega_{\underline{q},\underline{q}-\underline{k}} = -q^2[1-\rho_0 c(\underline{q})] + [\frac{1}{\rho_0}\delta\rho_{\rm gs}(\underline{q}-\underline{k}) - V^{\rm ex}_{uv}(\underline{q}-\underline{k})]\underline{q}\cdot(\underline{q}-\underline{k})$, the stability matrix.

Appendix C: Derivation of the scattering terms in the limit of low momentum transfer ($q\sigma \sim 0$)

The FT of $V_{uv}(\underline{r})$ is

$$\begin{aligned} V_{uv}(\underline{p}) &= \int \mathrm{d}\underline{r}\, \mathrm{e}^{i\underline{p}\cdot\underline{r}} V_{uv}(\underline{r}) = \int \mathrm{d}\underline{r} V_{uv}(\underline{r}) \left[1 + \frac{i\underline{p}\cdot\underline{r}}{1!} + \frac{(i\underline{p}\cdot\underline{r})^2}{2!} + \cdots\right] \\ &= \int \mathrm{d}\underline{r} V_{uv}(\underline{r}) \left[1 - ipr\cos\theta - \frac{(pr)^2\cos^2\theta}{2}\right] \\ &\quad \text{(higher-order terms neglected)} \\ &= \int \mathrm{d}r r^2 V(r) \int_0^\pi \sin\theta\,\mathrm{d}\theta \left[1 - ipr\cos\theta - \frac{(pr)^2\cos^2\theta}{2}\right] \int_0^{2\pi} \mathrm{d}\varphi \\ &= 4\pi \int \mathrm{d}r\, r^2 V_{uv}(r) - \frac{p^2}{2}\frac{4\pi}{3}\int \mathrm{d}r\, r^4 V_{uv}(r) = V_0 - \frac{p^2}{2}V_2, \end{aligned} \tag{C.1}$$

where

$$V_0 = 4\pi \int \mathrm{d}r\, r^2 V_{uv}(r) \quad \text{and} \quad V_2 = \frac{4\pi}{3}\int \mathrm{d}r\, r^4 V_{uv}(r). \tag{C.2}$$

Similarly,

$$c(\underline{p}) = C_0 - \frac{p^2}{2}C_2, \tag{C.3}$$

where

$$C_0 = 4\pi \int \mathrm{d}r\, r^2 c(\underline{r}) \quad \text{and} \quad C_2 = \frac{4\pi}{3}\int \mathrm{d}r\, r^4 c(\underline{r}).$$

In our case,

$$\beta V_{\rm gs}\left(\frac{r}{\sigma}\right) = -4\frac{\varepsilon}{k_{\rm B}T}\left(\frac{\sigma}{r}\right)^6 \quad \text{for} \quad \frac{r}{\sigma} > 1.$$

Hence, from eq. (C.1) we get

$$V^{(0)}_{\rm gs} = 4\pi \int_1^\infty \beta V^{\rm gs}_{uv}(r^*) r^{*2}\mathrm{d}r^* = 4\pi \int_1^\infty \left\{-4\varepsilon^* \frac{1}{r^{*6}}\right\} r^{*2}\mathrm{d}r^*$$

$$= -16\pi\varepsilon^* \int_1^\infty \frac{1}{r^{*4}} \mathrm{d}r^* = -\frac{16}{3}\pi\varepsilon^*,$$

$$V_{\mathrm{gs}}^{(2)} = \frac{4\pi}{3}\int_1^\infty \beta V_{uv}^{\mathrm{gs}}(r^*) r^{*4} \mathrm{d}r^* = \frac{4\pi}{3}\int_1^\infty \left\{-4\varepsilon^* \frac{1}{r^{*6}}\right\} r^{*4}\mathrm{d}r^*$$

$$= -\frac{16}{3}\pi\varepsilon^* \int_1^\infty \frac{1}{r^{*2}}\mathrm{d}r^* = -\frac{16}{3}\pi\varepsilon^*.$$

Therefore,

$$V_{\mathrm{gs}}^{(0)} = V_{\mathrm{gs}}^{(2)} = -\frac{16}{3}\pi\varepsilon^*$$

and

$$V_{\mathrm{ex}}^{(0)} = fV_{\mathrm{gs}}^{(0)} = -\frac{16}{3}\pi\varepsilon^* f = fV_{\mathrm{gs}}^{(2)} = V_{\mathrm{ex}}^{(2)}.$$

Here, for the correlation, we note that

$$c(r^*) = -\lambda_1 - 6\eta\lambda_2 r^* - \frac{1}{2}\eta\lambda_1 r^{*3} + 4\varepsilon^* \frac{1}{r^{*6}}.$$

Therefore, from eq. (C.2) we get

$$C_0 = 4\pi \int \mathrm{d}r^*\, r^{*2} c(r^*)$$

$$= -4\pi\lambda_1 \int_0^1 \mathrm{d}r^* r^{*2} - 4\pi 6\eta\lambda_2 \int_0^1 \mathrm{d}r^* r^{*3}$$

$$-4\pi\frac{1}{2}\eta\lambda_1 \int_0^1 \mathrm{d}r^* r^{*5} + 4\pi 4\varepsilon^* \int_1^\infty \mathrm{d}r^* r^{*2}\frac{1}{r^{*6}}$$

$$= -4\pi\lambda_1\frac{1}{3} - 24\pi\eta\lambda_2\frac{1}{4} - 2\pi\eta\lambda_1\frac{1}{6} + \frac{16}{3}\pi\varepsilon^*$$

$$= -V_{\mathrm{gs}}^{(0)} - \frac{1}{3}(\eta+4)\pi\lambda_1 - 6\pi\eta\lambda_2,$$

and

$$C_2 = \frac{4\pi}{3}\int \mathrm{d}r^* r^{*4} c(r^*)$$

$$= -\frac{4\pi}{3}\lambda_1 \int_0^1 \mathrm{d}r^* r^{*4} - \frac{4\pi}{3}6\eta\lambda_2 \int_0^1 \mathrm{d}r^* r^{*5}$$

$$-\frac{4\pi}{3}\frac{1}{2}\eta\lambda_1 \int_0^1 \mathrm{d}r^* r^{*7} + \frac{4\pi}{3}4\varepsilon^* \int_1^\infty \mathrm{d}r^* r^{*4}\frac{1}{r^{*6}}$$

$$= -\frac{4}{15}\pi\lambda_1 - \frac{4\pi}{3}\eta\lambda_2 - \frac{1}{12}\pi\eta\lambda_1 + \frac{16}{3}\pi\varepsilon^*$$

$$= -V_{\mathrm{gs}}^{(2)} - \frac{1}{3}\pi\lambda_1\left(\frac{4}{5} + \frac{1}{4}\eta\right) - \frac{4\pi}{3}\eta\lambda_2,$$

where

$$\eta = \frac{\pi}{6}\rho_0\sigma^3,\ \lambda_1 = (1+2\eta)^2/(1-\eta)^4,\ \lambda_2 = -\left(1+\frac{1}{2}\eta\right)^2/(1-\eta)^4,$$
$$r^* = \frac{r}{\sigma} \quad \text{and} \quad \varepsilon^* = \frac{\varepsilon}{k_{\mathrm{B}}T}.$$

Appendix D: Derivation of the expressions for the diagonal elements

In the $q\sigma \sim 0$ limit, we obtain

$$-q^2[1-\rho_0 c(q)] = \left[\rho_0\left\{C_0 - \frac{1}{2}q^2C_2\right\} - 1\right]q^2$$
$$= [\rho_0 C_0 - 1]q^2 - \frac{1}{2}\rho_0 C_2 q^4 = A^0_{\mathrm{st}}q^2 + B^0_{\mathrm{st}}q^4,$$

where $A^0_{\mathrm{st}} = -[1-\rho_0 C_0]$ and $B^0_{\mathrm{st}} = -\frac{1}{2}\rho_0 C_2$. For elastic scattering, the momentum transferred is $|\underline{q}-\underline{k}| = 2q\sin(\chi/2)$. Thus, for the ground state we can write

$$|\underline{q}-\underline{k}| = \frac{1}{\rho_0}2q^2\int\int \sin^2\frac{\chi}{2}\delta\rho_{\mathrm{gs}}\left(2q\sin\frac{\chi}{2}\right)\mathrm{d}(\cos\chi)\mathrm{d}\phi,$$

where ϕ is the azimuthal angle which is integrated over $0 \to 2\pi$; χ is the angle between the incident momentum and the scattered one. Therefore,

$$|\underline{q}-\underline{k}| = \frac{1}{\rho_0}2\pi q^2\int 2\sin^2\frac{\chi}{2}\delta\rho_{\mathrm{gs}}\left(2q\sin\frac{\chi}{2}\right)\mathrm{d}(\cos\chi)$$
$$= \frac{1}{\rho_0}2\pi q^2\int(1-\cos\chi)\delta\rho_{\mathrm{gs}}\left(2q\sin\frac{\chi}{2}\right)\mathrm{d}(\cos\chi). \qquad \text{(D.1)}$$

Now from eq. (3) we have

$$\delta\rho_{\mathrm{gs}}(\underline{p}) = \frac{-\beta\rho_0 V^{\mathrm{gs}}_{uv}(\underline{p})}{1-\rho_0 c(\underline{p})},$$

where $\underline{p} = 2\underline{q}\sin\frac{\chi}{2}$ and therefore

$$\delta\rho_{\mathrm{gs}}(\underline{p}) = -\rho_0\frac{1}{1-\rho_0\left[C_0 - \frac{1}{2}p^2C_2\right]}\left[V^{(0)}_{\mathrm{gs}} - \frac{p^2}{2}V^{(2)}_{\mathrm{gs}}\right]$$
$$= -\frac{\rho_0}{[1-\rho_0C_0]\left[1+\frac{1}{2}p^2\frac{\rho_0C_2}{1-\rho_0C_0}\right]}\left[V^{(0)}_{\mathrm{gs}} - \frac{p^2}{2}V^{(2)}_{\mathrm{gs}}\right]$$
$$= \frac{\rho_0}{(1-\rho_0C_0)}\left[1-\frac{1}{2}p^2\frac{\rho_0C_2}{1-\rho_0C_0}\right]\left[V^{(0)}_{\mathrm{gs}} - \frac{p^2}{2}V^{(2)}_{\mathrm{gs}}\right]$$
$$= -\frac{\rho_0}{[1-\rho_0C_0]}\left[V^{(0)}_{\mathrm{gs}} - \frac{1}{2}p^2\left[V^{(2)}_{\mathrm{gs}} + \frac{\rho_0C_2}{1-\rho_0C_0}V^{(0)}_{\mathrm{gs}}\right]\right]. \qquad \text{(D.2)}$$

For $q\sigma \sim 0$, all values of χ is possible and thus the limit of integration is $-1 \to +1$. Putting eq. (D.2) in eq. (D.1) and integrating over the limits we get contribution from ground state as

$$-4\pi \frac{V_{\rm gs}^{(0)}}{(1-\rho_0 C_0)} q^2 + \frac{16}{3}\pi \frac{1}{(1-\rho_0 C_0)} \left[V_{\rm gs}^{(2)} + \frac{\rho_0 C_2}{(1-\rho_0 C_0)} V_{\rm gs}^{(0)} \right] q^4. \quad \text{(D.3)}$$

Similarly, for $q\sigma \sim 0$, the contribution from the interaction potential can be given by

$$4\pi f V_{\rm gs}^{(0)} q^2 - \frac{16}{3}\pi f V_{\rm gs}^{(2)} q^4. \quad \text{(D.4)}$$

Hence, the total contribution from the scattering process is (using eqs (D.3) and (D.4))

$$\begin{aligned} &= -V_{\rm gs}^{(0)} \left[\frac{1}{1-\rho_0 C_0} + f \right] q^2 + \frac{4}{3} V_{\rm gs}^{(2)} \left[\frac{1}{1-\rho_0 C_0} + \frac{\rho_0 C_2}{(1-\rho_0 C_0)^2} + f \right] q^4 \\ &= A_{\rm sc}^{(0)} q^2 + B_{\rm sc}^{(0)} q^4, \end{aligned}$$

where

$$A_{\rm sc}^{(0)} = -V_{\rm gs}^{(0)} \left[\frac{1}{1-\rho_0 C_0} + f \right]$$

and

$$B_{\rm sc}^{(0)} = \frac{4}{3} V_{\rm gs}^{(2)} \left[\frac{1}{1-\rho_0 C_0} + \frac{\rho_0 C_2}{(1-\rho_0 C_0)^2} + f \right].$$

Note here that in $q\sigma \sim 0$ limit, the scattering term will be divided by 4π. Therefore, the total contribution to the diagonal element $\omega(\sigma^2/D) = A_{\rm G} q^2 + B_{\rm G} q^4$, where $A_{\rm G} = A_{\rm st}^{(0)} + A_{\rm sc}^{(0)}$ and $B_{\rm G} = B_{\rm st}^{(0)} + B_{\rm sc}^{(0)}$.

Appendix E: Derivation of the terms in the $q\sigma \sim 2\pi$ limit

For the ground state term, as C_2 is nearly flat at $q\sigma = q_0 = 2\pi$, we can safely ignore the term and thus

$$\delta\rho_{\rm gs}(p) = -\frac{\rho_0}{(1-\rho_0 C_0)} \left[V_{\rm gs}^{(0)} - \frac{p^2}{2} V_{\rm gs}^{(2)} \right] \text{ where } p = 2q \sin\frac{\chi}{2}.$$

Thus the contribution from the ground state is

$$-\frac{1}{4\pi^3} \frac{V_{\rm gs}^{(0)}}{(1-\rho_0 C_0)} q_0^2 + \frac{1}{12\pi^5} \frac{V_{\rm gs}^{(2)}}{(1-\rho_0 C_2)} q_0^4.$$

Similarly, the contribution from the interaction potential can be given by

$$\frac{1}{4\pi^3} f V_{\rm gs}^{(0)} q_0^2 - \frac{1}{12\pi^5} f V_{\rm gs}^{(2)} q_0^4.$$

Hence, the scattering term for the $q\sigma \sim q_0$ limit becomes

$$-\frac{1}{8\pi^3} V_{\rm gs}^{(0)} \left[\frac{1}{1-\rho_0 C_0} + f\right] q_0^2 + \frac{1}{24\pi^5} V_{\rm gs}^{(2)} \left[\frac{1}{1-\rho_0 C_0} + f\right] q_0^4$$
$$= A_{\rm sc}^{(2\pi)} q_0^2 + B_{\rm sc}^{(2\pi)} q_0^4,$$

where

$$A_{\rm sc}^{(2\pi)} = -\frac{1}{8\pi^3} V_{\rm gs}^{(0)} \left[\frac{1}{1-\rho_0 C_0} + f\right]$$

and

$$B_{\rm sc}^{(2\pi)} = \frac{1}{24\pi^5} V_{\rm gs}^{(2)} \left[\frac{1}{1-\rho_0 C_0} + f\right].$$

Here the scattering term is divided by a factor 2 that arises from $(4\pi/q_0) = (4\pi/2\pi) = 2$.

Thus the total diagonal contribution for the ordering wave vector ($q\sigma \sim q_0$) mode is $(\omega\sigma^2/D) = A_{\rm L} q_0^2 + B_{\rm L} q_0^4$, with $A_{\rm L} = A_{\rm st}(q \sim 2\pi) + A_{\rm sc}^{(2\pi)}$, $B_{\rm L} = B_{\rm sc}^{(2\pi)}$ and $A_{\rm st}(q \sim 2\pi) = -[1 - \rho_0 c(q \sim 2\pi)]$.

Acknowledgement

Financial assistance from the Department of Science and Technology (DST), India is gratefully acknowledged. SK thanks the S.N. Bose National Centre for Basic Sciences, Kolkata and the Indian Association for Cultivation of Science, Kolkata for providing a fellowship in the jointly conducted integrated Ph.D. in Chemical Sciences program.

References

[1] G R Fleming and P G Wolynes, *Phys. Today* **43**, 36 (1990)
[2] R F Grote and J T Hynes, *J. Chem. Phys.* **73**, 2715 (1980)
[3] J T Hynes, in *The theory of chemical reactions* edited bt M Baer (Chem. Rubber Publ. Co., Boca Raton, FL, 1985) Vol. 4
[4] B Bagchi and R Biswas, *Adv. Chem. Phys.* **109**, 207 (1999)
[5] D H Waldeck, *Chem. Rev.* **91**, 415 (1991)
[6] M Maroncelli *et al*, *J. Phys. Chem.* **B105**, 17311 (1995)
[7] T Pradhan and R Biswas, *J. Phys. Chem.* **A111**, 11514 (2007)
[8] T Pradhan and R Biswas, *J. Phys. Chem.* **A111**, 11524 (2007)
[9] R Biswas *et al*, *J. Phys. Chem.* **A112**, 915 (2008)
[10] B Bagchi, *Annu. Rev. Phys. Chem.* **40**, 115 (1989)
[11] B Bagchi and A Chandra, *Adv. Chem. Phys.* **80**, 1 (1999)
[12] B Bagchi, *J. Chem. Phys.* **100**, 506 (1994)

[13] M Maroncelli *et al*, *J. Phys. Chem.* **B100**, 10337 (1996)
[14] B M Ladanyi and S Nugent, *J. Chem. Phys.* **124**, 044505 (2006)
[15] S A Egorov, *Phys. Rev. Lett.* **93**, 023004-1 (2004)
[16] M Maroncelli *et al*, *J. Phys. Chem.* **A110**, 3405 (2006)
[17] R Biswas and J Chakrabarti, *J. Phys. Chem.* **B111**, 13743 (2007)
[18] B Bagchi *et al*, *J. Chem. Phys.* **108**, 4963 (1998)
[19] M C Cross and P Hohenberg, *Rev. Mod. Phys.* **65**, 851 (1993)
[20] J Chakrabarti, *J. Chem. Phys.* **118**, 249 (2003)
[21] B Bagchi, *Physica* **A145**, 273 (1987)
[22] U M B Marconi and P Tarazona, *J. Chem. Phys.* **110**, 8032 (1999)
[23] J P Hansen and I R McDonald, *Theory of simple liquids* 2nd edn (Academic Press, London, 1986)
[24] R Biswas and J Chakrabarti, unpublished results